

Doping evolution of antiferromagnetic order and structural distortion in $\text{LaFeAsO}_{1-x}\text{F}_x$

Q. Huang,¹ Jun Zhao,² J. W. Lynn,¹ G. F. Chen,³ J. L. Luo,³ N. L. Wang,³ and Pengcheng Dai^{2,4,*}

¹*NIST Center for Neutron Research, National Institute of Standards and Technology, Gaithersburg, MD 20899-6102, USA*

²*Department of Physics and Astronomy, The University of Tennessee, Knoxville, Tennessee 37996-1200, USA*

³*Beijing National Laboratory for Condensed Matter Physics, Institute of Physics, Chinese Academy of Sciences, P. O. Box 603, Beijing 100080, China*

⁴*Neutron Scattering Science Division, Oak Ridge National Laboratory, Oak Ridge, Tennessee 37831-6393, USA*

We use neutron scattering to study the structural distortion and antiferromagnetic (AFM) order in $\text{LaFeAsO}_{1-x}\text{F}_x$ as the system is doped with fluorine (F) to induce superconductivity. In the undoped state, LaFeAsO exhibits a structural distortion, changing the symmetry from tetragonal (space group $P4/nmm$) to orthorhombic (space group $Cmma$) at 155 K, and then followed by an AFM order at 137 K. Doping the system with F gradually decreases the structural distortion temperature, but suppresses the long range AFM order before the emergence of superconductivity. Therefore, while superconductivity in these Fe oxypnictides can survive in either the tetragonal or the orthorhombic crystal structure, it competes directly with static AFM order.

INTRODUCTION

A determination of the phase diagram in the FeAs-based $R\text{FeAsO}_{1-x}\text{F}_x$ (where $R = \text{La, Nd, Sm, Pr, ...}$) family of high-transition temperature (high- T_c) superconductors [1, 2, 3, 4, 5] is the first step necessary for a comprehensive understanding of their electronic properties. The parent compounds of these FeAs-based materials are nonsuperconducting semimetals. When cooling down from room temperature, $R\text{FeAsO}$ first exhibits a structural phase transition, changing the crystal symmetry from tetragonal (space group $P4/nmm$) to orthorhombic (space group $Cmma$), and then orders antiferromagnetically with a spin structure as shown in Figs. 1a and 1b [6, 7, 8, 9, 10, 11, 12]. While earlier work had shown that superconductivity induced by F-doping suppresses both the structural phase transition and static antiferromagnetic (AFM) order [6], how this process occurs in $R\text{FeAsO}_{1-x}\text{F}_x$ as a function of F-doping is still unclear. For example, in a systematic study of the F-doping dependence of the structural and magnetic phase diagram of $\text{CeFeAsO}_{1-x}\text{F}_x$, Zhao *et al.* [7] found that the Fe AFM order disappears before the appearance of superconductivity. However, it was not clear whether the orthorhombic structural distortion in the undoped compound is still present in the underdoped superconducting materials. On the other hand, while systematic X-ray diffraction experiments on $\text{SmFeAsO}_{1-x}\text{F}_x$ reveal that orthorhombic symmetry is present in the underdoped superconductors, there are no neutron scattering experiments to directly probe the AFM phase boundary in these materials [13]. Finally, recent μSR , transport, and Mössbauer experiments on the phase diagram of $\text{LaFeAsO}_{1-x}\text{F}_x$ suggest a first-order-like phase transition between the AFM and superconducting phases [14]. Furthermore, these authors argue that the tetragonal to orthorhombic structural phase transition is associated with the doping-induced AFM to superconductivity phase transition, a result clearly inconsistent with Ref.

[13].

The difficulty in obtaining a comprehensive phase diagram of $R\text{FeAsO}_{1-x}\text{F}_x$ stems from the fact that various local probes such as μSR and Mössbauer can detect magnetic long range order but are insensitive to the structural distortion [14]. On the other hand, X-ray scattering is sensitive to structural distortion but does not directly probe the AFM order. Neutron scattering is capable of detecting both structural and magnetic order, but requires large sample masses and therefore has only been done for a limited doping range in $\text{CeFeAsO}_{1-x}\text{F}_x$ [7]. In this paper, we present a systematic neutron scattering investigation of $\text{LaFeAsO}_{1-x}\text{F}_x$ that complements earlier work on this system [6, 8, 14]. Our data reveal that the orthorhombic structural distortion extends beyond the AFM phase and coexists with superconductivity, whereas there is no evidence of static long range AFM order coexisting with superconductivity.

EXPERIMENTAL RESULTS AND DISCUSSIONS

We use neutron diffraction to study the structural and magnetic phase transitions in polycrystalline samples of $\text{LaFeAsO}_{1-x}\text{F}_x$ with fluorine doping $x = 0, 0.03, 0.05,$ and 0.08 . Our experiments were performed on the BT-1 high resolution powder diffractometer and BT-7 triple axis spectrometer at the NIST Center for Neutron Research, Gaithersburg, Maryland. The BT-1 diffractometer has a $\text{Ge}(3,1,1)$ monochromator and an incident wavelength of $\lambda = 2.0785 \text{ \AA}$. Collimators with horizontal divergences of $15'$, $20'$, and $7'$ full-width-at-half-maximum (FWHM) were used before and after the monochromator, and after the sample, respectively. The BT-7 has a $\text{PG}(0,0,2)$ (pyrolytic graphite) monochromator with an incident beam wavelength of $\lambda = 2.359 \text{ \AA}$. A PG filter was placed in the incident beam path to eliminate $\lambda/2$ [6, 7]. The collimations are $50'$ FWHM before the sample and $80'$ radial collimator between the sample and a position

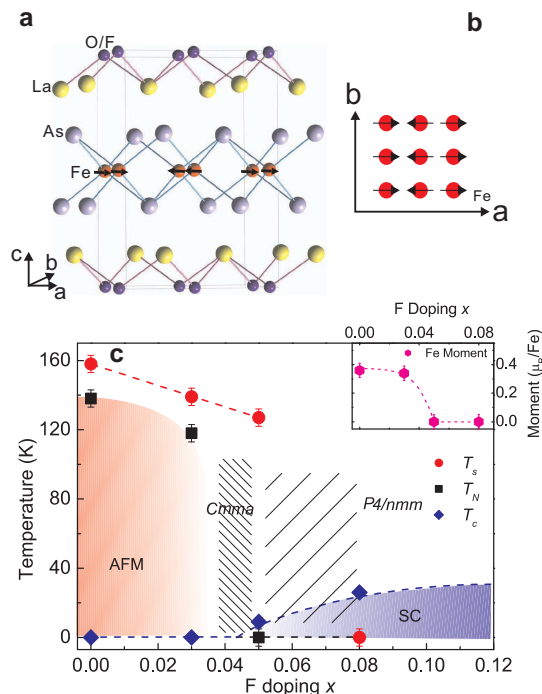


FIG. 1: (Color online) (a) The Fe spin ordering in the LaFeAsO chemical unit cell. (b) The Fe magnetic unit cell of LaFeAsO in the Fe-As plane. The Fe moments lie in the a - b plane along the a -axis and form an antiferromagnetic collinear spin structure similar to BaFe₂As₂, SrFe₂As₂, and CaFe₂As₂ [6, 7, 10, 12]. (c) The structural and magnetic phase diagram determined from our neutron measurements on LaFeAsO_{1-x}F_x with $x = 0, 0.03, 0.05, 0.08$. The red circles indicate the onset temperature of the $P4/nmm$ to $Cmma$ phase transition. The black squares designate the Néel temperatures of Fe as determined from neutron measurements in Fig. 3. The superconducting transition temperatures T_c for $x = 0.05, 0.08$ are determined from susceptibility measurements. The AFM to superconducting phase transition happens between $x = 0.03$ and 0.05 . The inset in d) shows the F doping dependence of the Fe moment as determined from the intensity of the $(1,0,3)_M$ magnetic peak at 4 K.

sensitive detector that covered an angular range of approximately five degrees. The polycrystalline samples of LaFeAsO_{1-x}F_x with $x = 0, 0.03, 0.05$, and 0.08 were prepared by the solid state reaction using LaAs, Fe₂O₃, Fe and LaF₃ as starting materials, with the detailed preparation method described in Ref. [16]. We checked the superconducting properties of each LaFeAsO_{1-x}F_x using a SQUID magnetometer and found that the $x = 0, 0.03$ samples are nonsuperconducting, while the $x = 0.05$ and 0.08 samples are 8 K and 26 K superconductors, respectively. The fluorine-doping levels are nominal, and should be close to the actual electron-doping level at these concentrations.

Figures 1a and 1b show the Fe spin structure within the FeAs layer as determined from previous neutron scat-

TABLE I: Refined crystal structure parameters of LaFeAsO_{1-x}F_x with $x = 0$ at 175 K ($R_p = 5.24\%$, $w_{Rp} = 6.62\%$, $\chi^2 = 0.9825$), and $x = 0.08$ at 10 K ($R_p = 5.05\%$, $w_{Rp} = 6.6\%$, $\chi^2 = 0.9273$). Space group: $P4/nmm$. LaFeAsO, $a = 4.03007(9)$, $c = 8.7368(2)$ Å; LaFeAsO_{0.92}F_{0.08}, $a = 4.02005(4)$, $c = 8.7032(1)$ Å.

Atom	site	x	y	z(x = 0)	z(x = 0.08)
La	2c	$\frac{1}{4}$	$\frac{1}{4}$	0.1417(3)	0.1450(3)
Fe	2b	$\frac{3}{4}$	$\frac{1}{4}$	$\frac{1}{2}$	$\frac{1}{2}$
As	2c	$\frac{1}{4}$	$\frac{1}{4}$	0.6507(4)	0.6520(3)
O	2a	$\frac{3}{4}$	$\frac{1}{4}$	0	0

tering work on RFeAsO [6, 7, 8] and (Ba,Sr,Ca)Fe₂As₂ [10, 11, 12]. Figure 1c summarizes the electronic phase diagram of LaFeAsO_{1-x}F_x determined from our measurements. Our data are consistent with previous neutron scattering [6] and results from local probes such as μ SR and ⁵⁷Fe Mössbauer spectroscopy [14], and indicates that long range AFM order disappears as a function of doping before superconductivity is present. On the other hand, we find direct evidence for the orthorhombic structural distortion in the underdoped superconducting LaFeAsO_{1-x}F_x, indicating that the orthorhombic lattice distortion extends into the superconductivity dome in LaFeAsO_{1-x}F_x, similar to that of SmFeAsO_{1-x}F_x [13].

To demonstrate this, we show in Figure 2a a comparison of the high-resolution BT-1 data for LaFeAsO_{1-x}F_x with $x = 0, 0.03, 0.05$, and 0.08 taken at 4 K. While the parent compound LaFeAsO shows clear evidence of the orthorhombic lattice distortion as illustrated by the splitting of the $(4, 0, 0)_o$ and $(0, 4, 0)_o$ peaks, doping F gradually reduces the splitting of these peaks until they become a single resolution-limited peak corresponding to tetragonal symmetry for $x = 0.08$ [6]. For $x = 0.03$, one can see a clear splitting of the $(4, 0, 0)_o$ and $(0, 4, 0)_o$ peaks. Although a well-resolved splitting is no longer observable in the $x = 0.05$ sample, the peak width is broader than the resolution-limited case of $x = 0.08$ (Fig. 2a). In particular, we note that the width of the $(0, 0, 6)$ peak, which is not sensitive to the in-plane lattice distortion, is resolution limited for all concentrations. Hence the peak broadening for the in-plane peaks of the $x = 0.05$ sample must arise from the underlying orthorhombic structure. In addition, we would expect that the temperature dependence of the $(2, 2, 0)_T$ reflection peak intensity (not integrated intensity) measured by the high-resolution BT-1 should decrease going through the tetragonal to orthorhombic symmetry change. Figures 2b-d show that this is indeed the case, where the tetragonal to orthorhombic symmetry change temperature reduces systematically as a function of increasing F-doping.

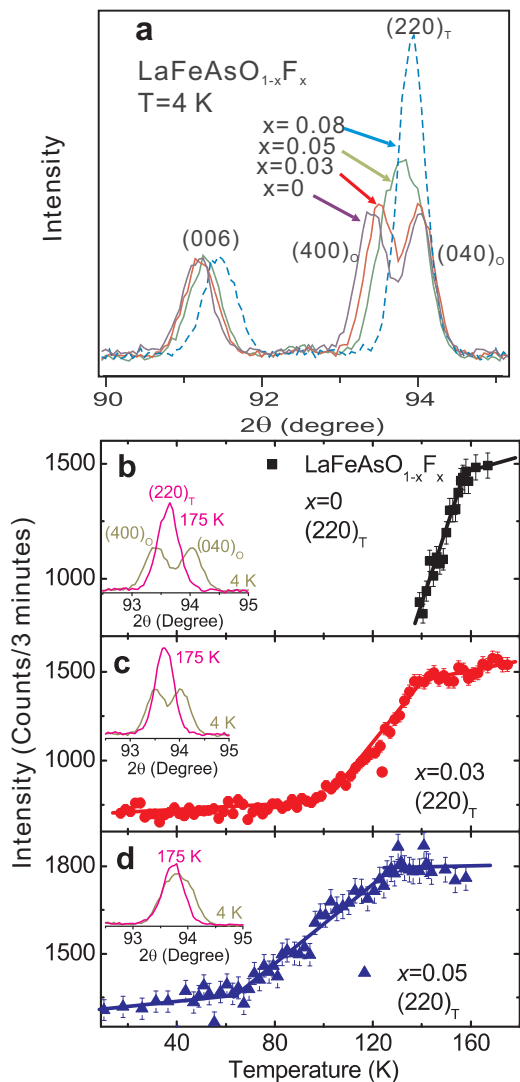


FIG. 2: (Color online) Dependence of the low-temperature crystal structure of $\text{LaFeAsO}_{1-x}\text{F}_x$ as a function of F-doping x . (a) 2θ scans, showing the reduction of the orthorhombic lattice distortion with increasing F-doping. The $(2, 2, 0)$ peak for $x = 0.05$ is clearly broader than the resolution. (b-d) Temperature dependence of the $(2, 2, 0)_T$ (T denotes tetragonal) nuclear reflection indicative of a structural phase transition for various x [6]. The temperature of the tetragonal to orthorhombic lattice distortion reduces with increasing x . The insets show the $(2, 2, 0)_T$ reflection above and below the transition temperatures.

Figure 3 summarizes the F-doping dependence of the AFM Bragg peak and magnetic order parameter. μSR measurements on $\text{LaFeAsO}_{1-x}\text{F}_x$ with $x = 0, 0.03$ [15] confirmed that the undoped parent LaFeAsO compound has static AFM order, but the 3% F-doping might induce an incommensurate/stripe-like AFM magnetic order. To determine the F-doping dependence of the AFM order, we probed the $(1, 0, 3)$ magnetic peak. Figure 3a plots the wave vector dependence of the $(1, 0, 3)$ at 2 K. When

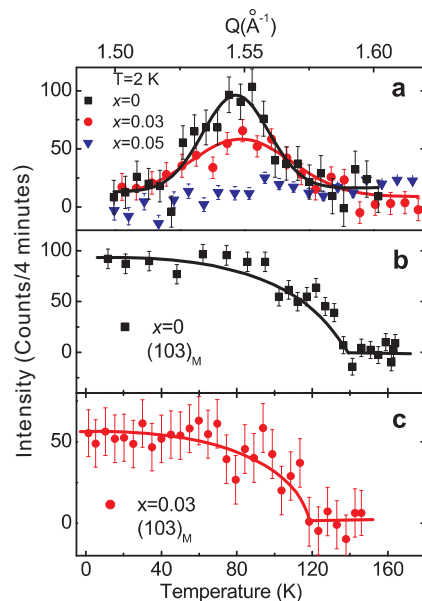


FIG. 3: (Color online) (a) Wave vector dependence of the AFM ordering peak $(1, 0, 3)$ for $x = 0, 0.03, 0.05$ at 2 K. The intensity of scattering is normalized to the nuclear Bragg peaks and can be compared directly. (b,c) Temperature dependence of the magnetic scattering for $x = 0, 0.03$, respectively.

3% F is introduced, the $(1, 0, 3)$ peak becomes weaker and broader. The broadening can be interpreted as a reduction in the Fe spin-spin correlation length from $208 \pm 28\text{ \AA}$ for $x = 0$ to $139 \pm 33\text{ \AA}$ for $x = 0.03$, with the scattering still being commensurate and centered at $(1, 0, 3)$ for both materials. This broadening is somewhat different from the doping-dependent magnetic scattering for $\text{CeFeAsO}_{1-x}\text{F}_x$ [7], where the magnetic peaks at finite F-dopings were always resolution-limited. This suggests that the broadening might be interpreted as originating from incommensurate AFM magnetic order, with an incommensurability that cannot be resolved. Future experiments on single crystals should be able to resolve this issue. On further increasing the F-doping to $x = 0.05$, where superconductivity with $T_c = 8\text{ K}$ is induced, the $(1, 0, 3)$ static AFM ordering peak is no longer observable (Fig. 3a). Therefore, while the orthorhombic lattice distortion extends to samples with bulk superconductivity, static AFM order does not coexist with superconductivity within the accuracy of our measurements [17].

Figures 3b and 3c show the temperature dependence of the $(1, 0, 3)$ peak intensity. Consistent with previous neutron scattering [6, 8] and μSR work [14, 15], the Néel temperatures of $\text{LaFeAsO}_{1-x}\text{F}_x$ with $x = 0, 0.03$ are 137 ± 3 and $120 \pm 2\text{ K}$, respectively. Figure 1c summarizes the structural and magnetic phase diagram determined from the present work. One of the key differences between the present phase diagram and that determined by μSR and Mössbauer effect measurements [14] is the presence of

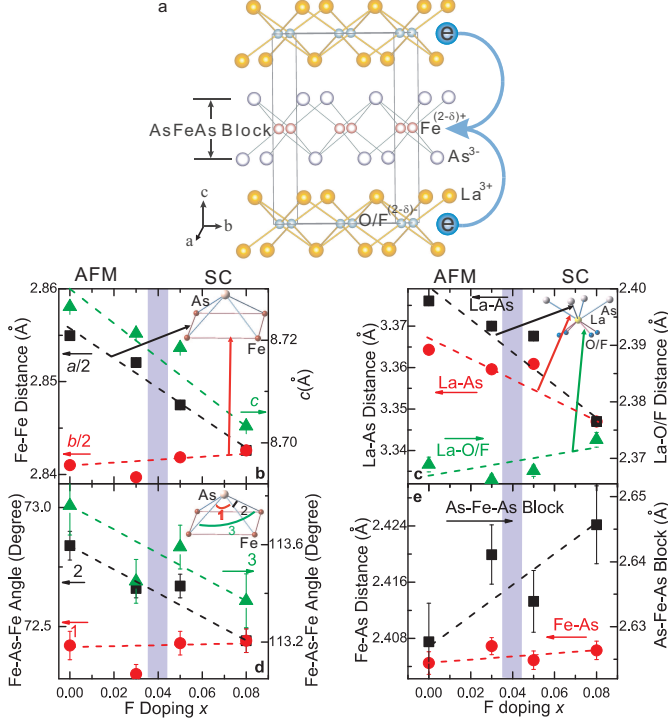


FIG. 4: (Color online) Low temperature structural evolution of $\text{LaFeAsO}_{1-x}\text{F}_x$ as a function of F doping obtained from analysis of the BT-1 data. There is no sudden structural transition as the AFM order is replaced by the superconducting phase. The atomic positions of $\text{LaFeAsO}_{1-x}\text{F}_x$ and their temperature dependence are shown in Tables I and II. (a) schematic diagram defining the As-Fe-As block and illustrating the process of electron doping. (b) a , b , c lattice constants of the orthorhombic unit cell and the two Fe-Fe nearest-neighbor distances as a function of F doping. Similar to $\text{CeFeAsO}_{1-x}\text{F}_x$, F-doping only suppresses the long-axis of the orthorhombic structure. (c) La-O/F and La-As distances as a function of F doping. The slight increase in the La-O/F block size is compensated by a much larger reduction in the La-As distance, resulting in an overall c -axis lattice contraction as shown in (b). (d) Fe-As-Fe bond angles as defined in the inset versus F doping. While angle 1 hardly changes with doping, angles 2 and 3 decrease substantially with increasing F doping. (e) The Fe-As bond distance and As-Fe-As block size versus F doping. The Fe-As distance is independent of F doping.

the orthorhombic lattice distortion in underdoped superconducting $\text{LaFeAsO}_{1-x}\text{F}_x$. This indicates that the evolution from antiferromagnetism to superconductivity is not directly associated with the tetragonal to orthorhombic structural phase transition. Instead, our data appear to support the idea that commensurate AFM order is a competing ground state to superconductivity, much like the case of electron-doped high- T_c copper oxides [18, 19]. Theoretically, it has been argued that the orthorhombic lattice distortion in $\text{RFeAsO}_{1-x}\text{F}_x$ is associated with nematic ordering of the Fe spin fluctuations and therefore

TABLE II: Refined crystal structure parameters of $\text{LaFeAsO}_{1-x}\text{F}_x$ with $x = 0, 0.03, 0.05$ at 2 K. Space group: $Cmma$. Atomic positions: La: $4g(0, \frac{1}{4}, z)$; Fe: $4b(\frac{1}{4}, 0, \frac{1}{2})$; As: $4g(0, \frac{1}{4}, z)$; and O/F: $4a(\frac{1}{4}, 0, 0)$.

Atom	$x = 0$	$x = 0.03$	$x = 0.05$	
$a(\text{\AA})$	0.50988(9)	5.70407(8)	5.6995(2)	
$b(\text{\AA})$	5.68195(9)	5.67936(8)	5.6837(2)	
$c(\text{\AA})$	8.7265(1)	8.7213(1)	8.7185(1)	
La	z	0.1430(3)	0.1427(2)	0.1431(2)
As	z	0.6506(3)	0.6514(3)	0.6510(3)
$R_p(\%)$	4.26	4.36	5.21	
$w_{Rp}(\%)$	5.47	5.75	6.87	
χ^2	1.005	0.9327	1.221	

is a precursor of long range AFM order [20, 21, 22].

Previous systematic work on $\text{CeFeAsO}_{1-x}\text{F}_x$ [7] found that the impact of F-doping is to compress the c - and a - axes of the orthorhombic structure, where $c > a > b$, while leaving the b -axis unchanged. The decrease in the c -axis lattice constant is mostly due to the distance reduction of the CeO and FeAs blocks. To see if this is also true for $\text{LaFeAsO}_{1-x}\text{F}_x$, we plot the doping dependence of the Fe-Fe distance (Fig. 4b), La-As and La-O/F distances (Fig. 4c), Fe-As-Fe bond angles (Fig. 4d), and Fe-As/As-Fe-As block distances (Fig. 4e) obtained from detailed analysis of the high-resolution BT-1 data (see Tables 1 and 2 for details). Consistent with earlier work on $\text{CeFeAsO}_{1-x}\text{F}_x$ [7], we find that electron doping suppresses the long a -axis of the orthorhombic structure while leaving the short b -axis unchanged. Similarly, doping electrons reduces the distance between the LaO and FeAs blocks, mostly likely due to increased Coulomb attraction between these two blocks. Since the Fe-As distance (2.404 Å) is essentially doping independent (Fig. 4e), the net effect of the a -axis lattice contraction is to push the diagonal Fe-As-Fe angle toward the ideal value of 109.47° for the perfect FeAs tetrahedron (Fig. 4d). The lattice structure is seen to evolve smoothly across the AFM to superconductivity phase transition. These results confirm the notion that the most effective way to increase T_C in Fe-based superconductors is to decrease the deviation of the Fe-As(P)-Fe bond angle from the ideal FeAs tetrahedron [7, 23].

CONCLUSIONS

In summary, we have shown that the orthorhombic lattice distortion present in undoped LaFeAsO can extend beyond the AFM to superconductivity phase boundary, whereas the static long-range AFM ordered phase does not seem to coexist with superconductivity. The phase diagram of electron-doped LaFeAsO_{1-x}F_x can therefore be sketched as in Fig. 1c, showing clear coexistence of superconductivity with either the orthorhombic or tetragonal lattice structure.

ACKNOWLEDGMENTS

This work is supported by the US NSF through DMR-0756568, by the US DOE, Division of Materials Science, Basic Energy Sciences, through DOE DE-FG02-05ER46202. This work is also supported in part by the US DOE, Division of Scientific User Facilities, Basic Energy Sciences. The work at the Institute of Physics, Chinese Academy of Sciences, is supported by the NSF of China, the Chinese Academy of Sciences and the Ministry of Science and Technology of China.

* Electronic address: daip@ornl.gov

- [1] Y. Kamihara, T. Watanabe, M. Hirano, and H. Hosono, *J. Am. Chem. Soc.* **130**, 3296 (2008).
- [2] X. H. Chen, T. Wu, G. Wu, R. H. Liu, H. Chen, and D. F. Fang, *Nature (London)* **453**, 761 (2008).
- [3] G. F. Chen, Z. Li, D. Wu, G. Li, W. Z. Hu, J. Dong, P. Zheng, J. L. Luo, and N. L. Wang, *Phys. Rev. Lett.* **100**, 247002 (2008).
- [4] Zhi-An Ren, G. Che, X. Dong, J. Yang, W. Lu, W. Yi, X. Shen, Z. Li, L. Sun, F. Zhou and Z.X. Zhao, *Europhys. Lett.* **83**, 17002 (2008).
- [5] H. H. Wen, G. Mu, L. Fang, H. Yang and X. Zhu, *Europhys. Lett.* **82**, 17009 (2008).
- [6] C. de la Cruz, Q. Huang, J. W. Lynn, J. Li, W. Ratcliff II, J. L. Zarestky, H. A. Mook, G. F. Chen, J. L. Luo, N. L. Wang, Pengcheng Dai, *Nature (London)* **453**, 899 (2008).
- [7] Jun Zhao, Q. Huang, C. de la Cruz, Shiliang Li, J. W. Lynn, Y. Chen, M. A. Green, G. F. Chen, G. Li, Z. Li, J. L. Luo, N. L. Wang, Pengcheng Dai, arxiv.org/abs/0806.2528.
- [8] M. A. McGuire, A. D. Christianson, A. S. Sefat, B. C. Sales, M. D. Lumsden, R. Jin, E. A. Payzant, D. Mandrus, Y. Luan, V. Keppens, V. Varadarajan, J. W. Brill, R. P. Hermann, M. T. Sougrati, F. Grandjean, G. J. Long, arxiv.org/abs/0806.3878.
- [9] Y. Chen, J. W. Lynn, J. Li, G. Li, G. F. Chen, J. L. Luo, N. L. Wang, Pengcheng Dai, C. dela Cruz, H. A. Mook, *Phys. Rev. B* **78**, 064515, (2008).
- [10] Q. Huang, Y. Qiu, Wei Bao, J.W. Lynn, M.A. Green, Y. Chen, T. Wu, G. Wu, X.H. Chen, arxiv.org/abs/0806.2776.
- [11] Jun Zhao, W. Ratcliff II, J. W. Lynn, G. F. Chen, J. L. Luo, N. L. Wang, J. Hu, Pengcheng Dai, arxiv.org/abs/0807.1077.
- [12] A.I. Goldman, D.N. Argyriou, B. Ouladdiaf, T. Chatterji, A. Kreyssig, S. Nandi, N. Ni, S. L. Bud'ko, P.C. Canfield, R. J. McQueeney, arxiv.org/abs/0807.1525.
- [13] S. Margadonna, Y. Takabayashi, M. T. McDonald, M. Brunelli, G. Wu, R. H. Liu, X. H. Chen, K. Prassides, arxiv.org/abs/0806.3962.
- [14] H. Luetkens, H.-H. Klauss, M. Kraken, F. J. Litterst, T. Dellmann, R. Klingeler, C. Hess, R. Khasanov, A. Amato, C. Baines, J. Hamann-Borrero, N. Leps, A. Kondrat, G. Behr, J. Werner, B. Buechner, arxiv.org/abs/0806.3533.
- [15] J.P. Carlo, Y.J. Uemura, T. Goko, G.J. MacDougall, J.A. Rodriguez, W. Yu, G.M. Luke, Pengcheng Dai, N. Shannon, S. Miyasaka, S. Suzuki, S. Tajima, G.F. Chen, W.Z. Hu, J.L. Luo, N.L. Wang, arxiv.org/abs/0805.2186.
- [16] G. F. Chen, Z. Li, G. Li, J. Zhou, D. Wu, J. Dong, W. Z. Hu, P. Zheng, Z. J. Chen, H. Q. Yuan, J. Singleton, J. L. Luo, and N. L. Wang, *Phys. Rev. Lett.* **101**, 057007 (2008).
- [17] In a recent μ SR work, Takeshita *et al.* [arxiv.org/abs/0806.4798v1.] suggest that weak spin-glass-like magnetism coexists with superconductivity in a LaFeAsO_{1-x}F_x $x = 0.06$ sample. Since neutron measurements present here are sensitive only to static long range order, our data do not eliminate the possibility of short-range, spin-glass-like, magnetic correlations coexists with superconductivity.
- [18] H. J. Kang, P. Dai, H. A. Mook, D. N. Argyriou, V. Sikolenko, J. W. Lynn, Y. Kurita, S. Komiya, and Y. Ando, *Phys. Rev. B* **71**, 214512 (2005).
- [19] S. D. Wilson, Shiliang Li, Jun Zhao, G. Mu, Hai-hu Wen, Jeffrey W. Lynn, Paul G. Freeman, Louis-Pierre Regnault, Klaus Habicht, Pengcheng Dai, *PNAS* **104**, 15259 (2007).
- [20] C. Fang, H. Yao, W.-F. Tsai, J. P. Hu, and S. A. Kivelson, *Phys. Rev. B* **77**, 224509 (2008).
- [21] C. Xu, M. Müller, and S. Sachdev, *Phys. Rev. B* **78**, 020501(R) (2008).
- [22] C. Xu, Y. Qi, and S. Sachdev, arxiv.org/abs/0807.1542v1.
- [23] C. H. Lee, A. Iyo, H. Eisaki, H. Kito, M. T. Fernandez-Diaz, T. Ito, K. Kihou, H. Matsuhata, M. Braden, K. Yamada, arxiv.org/abs/0806.3821v2.